MAGMA (2005) 18: 19–25
DOI 10.1007/s10334-004-0074-4

RESEARCH ARTICLE

P. M. Gonçalves Pereira
E. Oliveira
M. F. Secca

Assessment of the preferred scout sagittal orientation for temporal lobe imaging with magnetic resonance

Received: 17 May 2004
Revised: 12 July 2004
Accepted: 7 September 2004
Published online: 3 December 2004

P. M. Gonçalves Pereira (✉)
Department of Neuroradiology,
'Egas Moniz' Hospital,
Rua da Junqueira 126
1349-019 Lisboa Portugal
E-mail: pmgp@fct.unl.pt
Tel.: +351-21-3031140,
Fax: +351-21-3018140,

P. M. Gonçalves Pereira
Department of Medical Science,
Medical School,
University of Beira Interior,
Polo I, Rua Marquês d'Ávila e Bolama
6201-001 Covilhã
Portugal

P. M. Gonçalves Pereira · M. F. Secca
Department of Physics, CEFITEC,
School of Science and Technology,
New University of Lisboa,
Quinta da Torre 2825-114
Monte de Caparica
Portugal

E. Oliveira
Departement of Statistics,
'Egas Moniz' CRL,
Health Science Institute (ISCS),
Campus Universitário,
Quinta da Granja 2829-511
Monte de Caparica
Portugal

M. F. Secca
'Caselas' Magnetic Resonance Center,
Rua Carolina Ângelo,
1400-045 Lisboa
Portugal

Abstract Oblique magnetic resonance imaging of the temporal lobe (tilted orientation) requires a stable reference line with minimum variability. In the clinical setting, where several observers carry out examination of the patients, there is a need to assure minimum inter-observer variability, in order to obtain comparable tilted anatomical planes. This is particularly relevant when performing quantitative imaging (qMRI) of the hippocampus, amygdala and para-hippocampal cortices. In this study, eight experienced observers tested the stability of four sagittal reference lines by manually tracing the posterior commissure-obex (PC-OB) line, the line tangential to the anterior surface of the pons at its most convex point and the lines orthogonal to the main axis of both hippocampi, in ten exams of healthy subjects. The stability of the tracing was assessed by comparing the inter-observer variability expressed by the variances of the measurements. The observers' performance was assessed by comparing the precision of the tracing for each line. We tested the results statistically using Bartlett's test (analysis of the variances of the four lines) followed by Fischer–Snedecor (in order to compare the two lines that had the smallest variance). The PC-OB line and the line tangential to the anterior surface of the pons had smaller inter-observer variances than the orthogonal lines ($p < 0.01$). In addition, the variance of the PC-OB line was smaller than that of the line tangential to the pons ($p < 0.01$). There were no significant intra-observer differences in the precision of tracing of any of the lines. We show quantitatively that the PC-OB line is the scout reference that yields the smallest inter-observer variance. Thus, this line should be preferred to improve the reproducibility of temporal lobe imaging while performing tilted coronal and axial sequences, to make quantitative assessments of the hippocampus, amygdala and para-hippocampal cortices.

Introduction

The temporal lobe is the main target structure of temporal lobe epilepsy (TLE) [1], Alzheimer-type dementia [2], memory disturbances [3], including mild cognitive deficits [4], schizophrenia [5] and brain trauma [6]. In neurodegenerative disorders and epilepsy, the core limbic structures of the temporal lobe, that is, the hippocampus, the amygdala and the para-hippocampal cortex (see [7] for a review) are particularly affected.

Magnetic resonance imaging (MRI) is an essential tool to evaluate the abnormalities of even the smallest brain structures, due to its non-invasive multi-planar capabilities. Currently, qualitative and quantitative MRI is often used to study mesial temporal areas. Qualitative assessments are based on morphological and signal intensity appearances and depend heavily on the expertise of the radiologist. Quantitative imaging (qMRI) yields numerical information (for example: volumes, relaxation times, water diffusibility, metabolite concentration, blood perfusion measurements) that can be compared with normative values, but it depends on the identification of exact anatomical landmarks in order to be reproducible (see [8] for a review). Therefore, to be able to compare different MRIs and to perform serial or longitudinal studies, using either visual inspection or qMRI, it is essential that the landmarks of cross-sectional images are unambiguously defined.

Selective hippocampal atrophy can be found in patients with intractable partial seizures [9], Alzheimer-type dementia [10], amnesic syndromes [11] or schizophrenia [12]. In the pathophysiology of TLE, it is assumed that the degree of hippocampal, amygdala and para-hippocampal atrophy associates with the magnitude of neuronal loss [9], as the amount of reactive hippocampal astrocytes correlates with the measured T2-relaxometry times [13]. Hippocampal damage can also be detected by spectroscopy [14]. Morphological criteria, including indirect signs are also important to detect hippocampal or amygdala sclerosis. Subtle loss of the digitations of the hippocampal head [15], disruption of the internal architecture [16] and fornix and mamillary bodies' atrophy [17] are reliable indicators of hippocampal damage. Signal changes are also common in the hippocampus and amygdala of TLE patients [16, 18]. Thus, early and accurate diagnosis depends on the ability to identify small variations in the structures' volume, morphology and signal intensity.

The orientation of the acquired images, along with the criteria used for MR analysis and the knowledge of normal and abnormal mesial temporal lobe anatomy are key factors for the interpretation of MR images. Moreover, in qMRI one should assure reproducibility of the measurements by taking a constant tilted orientation to the temporal lobe in successive exams, minimizing in this way, partial volume effects.

Different MR sequences, including several anatomical planes have been used to evaluate the mesial temporal lobe [19]. One preferential anatomical orientation is the tilted coronal plane obtained at right angles to the main hippocampal axis [19–21]. For volumetric and relaxometric studies of the hippocampus and amygdala this is the plane mostly used, while multi-voxel spectroscopy benefits most if performed on a tilted axial orientation perpendicular to this angled coronal view [14, 20, 22].

In order to define a suitable and stable anatomical guideline for temporal lobe MRI studies, and to find out which reference line corresponds to the smallest inter-observer variation, we examined how eight different observers performed with respect to four different sagittal reference lines in ten MR exams of healthy persons. Two of the lines tested are commonly used as scouts of MR studies of the temporal lobe, that is, the lines perpendicular to the main axes of both hippocampi [19, 20] (either the right or left hippocampal body). The other two, the posterior commissure-obex (PC-OB) line and the line tangential to the anterior surface of the pons at its most convex point, have been also proposed as appropriate references in some studies [23, 24].

Materials and methods

Test subjects

The test group included ten subjects (five women) with a mean age [± 1 standard deviation (SD)] of 31.6 ± 3.2 (range: 27–36) years. All the volunteers were interviewed to exclude those with neurologic diseases and were submitted to detailed neurological examination and a "mini-mental state" test [25] [obtained mean score ± 1 SD and range was: 28.4 ± 1.3 (27–30)].

Test observers

Eight different observers with a mean number of years of experience of MRI work of 10.6 ± 6.5 (range: 2–17), volunteered to trace manually the chosen reference lines on a set of sagittal images, since this is the scout plane which is mostly used to define the coronal and axial sequences.

MR image acquisition and processing

All imaging studies were obtained on the same 1.5-T scanner (GE CV/i–NV/i. General Electric, Milwaukee, WI).

A standard sagittal spin-echo T1-weighted sequence, covering the whole brain was obtained with TR = 600 ms, TE = 15 ms, NEX = 2, FOV = 24 cm, section thickness = 5 mm, gap = 1 mm and acquisition matrix = 512×192 pixels.

Standard whole-brain coronal T1 and T2 images and axial T2 were acquired to exclude any structural abnormality.

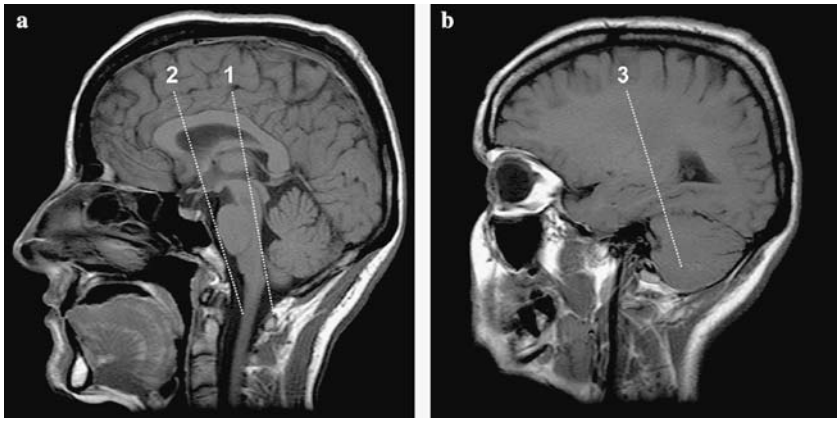

Fig. 1 Sagittal MR images demonstrate the location of three of the four lines tested. (a) mid-sagittal level showing the posterior commissure-obex line [1] and the line tangential to the anterior surface of the pons [2] (b) para-sagittal image showing the line orthogonal to the long axis of the right hippocampus [3]. The fourth line was orthogonally placed on the opposite hippocampus

Imaging processing was performed with the manufacturer's software GE Advantage Windows 3.1 (Viewer module), running on a workstation (SPARC 4.1, Sun Microsystems, Mountain View, Calif.). The software uses a graphical interface that allows to perform measurements (areas, lengths and angles). The measurements are displayed directly in absolute values (mm^2, mm or degrees), benefiting from the automatic calibration performed at the MR scanner during the acquisition of the images. For every graphic element introduced on top of an image, the software calculates automatically the measured values, which are shown on the workstation with the correspondent spatial coordinates.

Reference lines and coordinate system

Four anatomical lines (Fig. 1) were chosen to test the inter-observer variability. These lines represent standard references and anatomical axes used in daily practice [23].

Line 1 (k_1), connects the posterior commissure to the obex of the IV ventricle (PC-OB), joining two well-recognizable anatomical structures.

Line 2 (k_2), was marked tangentially to the anterior surface of the pons, at the point where the surface has maximal convexity.

Lines 3 (k_3) and 4 (k_4) were marked at right angles to the main axis of the hippocampal bodies, respectively in the right and the left hippocampus, as indicated by Watson et al. [20].

After tracing each anatomical line, the value of the angle (α- in degrees) between k and the vertical axis (set at zero degrees – see Fig. 2) was displayed directly on the workstation. The angles are calculated in relation to the vertical axis on the workstation screen and the value that is obtained measures the tilt of the line draw relatively to zero degrees (0°). The origin of the coordinate system (the center, where the three main axes cross zero) and the directions of these axes are defined with respect to the magnet's geometry. The center is defined as the geometric center of the magnetic field. The axes are defined as superior-inferior, anterior-posterior and left-right. The superior-inferior axis is defined as the line passing through the center and parallel to the main axis of the magnetic field, which is parallel to the basis of the magnet (and longitudinal to the scanner). The anterior-posterior axis is perpendicular to the superior-inferior axis, passing through the center, and perpendicular to the basis of the magnet. The left-right axis is perpendicular to the superior-inferior axis, passing through the center, and parallel to the basis of the magnet. The directions of the axes are characterized by the position of the subject in the scanner. In our case, the subjects were introduced head first and supine (and centered with the aid of the scanner's laser-cross beam). Therefore, superior-inferior is directed anatomically from head to feet, anterior-posterior from the back of the head to the nose and left-right is directed to the left-right of the subject.

The mean and the standard deviation of the angles for each anatomical line obtained in each test-subject MRI were further calculated.

Since each test subject underwent only one examination and the observers used the same sagittal image sets from each volunteer to mark the lines $k_1 - k_4$, the tilt of the head of the test subjects does not influence the results. We were specifically interested in studying the relative variances of these anatomical lines, not their absolute αvalues.

Statistical analysis

For the four lines, the mean and standard deviation of the angles as defined above (Fig. 2) were computed for each test subject and by each observer as indicated by Eq. 1 and 2:

$$S_{kj}^2 = \sum_{i=1}^{n_i} \left(\frac{\alpha_{kij} - \bar{\alpha}_{kj}}{n_i - 1} \right)^2 \quad (1)$$

$$S_k^2 = \sum_{j=1}^{n_j} \frac{S_{kj}^2}{n_j} \quad (2)$$

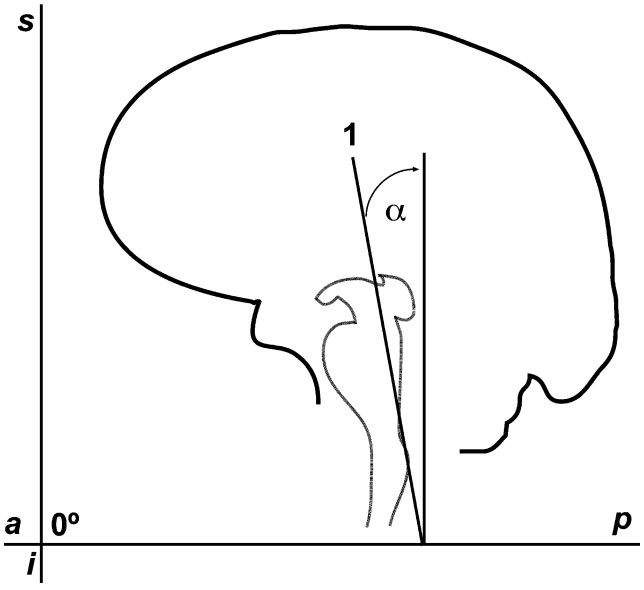

Fig. 2 Schematic drawing illustrates the angle α obtained from line 1 – posterior commissure-obex – in a sample case. Two of the axes of the coordinate system are depicted on the left side of the figure; *a –p*, on the horizontal line, represent the anterior–posterior axis and *s-i*, on the vertical line, corresponds to the superior-inferior axis. The value of α is calculated in regard to the anterior-posterior axis (zero degrees)

where

S_{kj}^2 - inter-observer variance of the angle for line k for a given test-subject j
n_i - number of observers
α_{kij} - value of the angle (relative to the vertical axis) measured by observer i for the test-subject j with respect to the line k
$\bar{\alpha}_{kj}$ - mean of the values of the angle with respect to line k for all observers for a given test-subject j
S_k^2 - mean of the variances for all test subjects with respect to line k (inter-subject variance for line k)
n_j - number of test subjects

The line with the smallest inter-observer variance S_k^2 of the angle α was considered the most stable. Differences in stability of the four lines were tested using Bartlett's test comparing S_k^2 with the mean total variance S^2 for all lines obtained by equation (3):

$$S^2 = \sum_{k=1}^{n_k} \frac{S_k^2}{n_k} \tag{3}$$

where

n_k - number of lines

The two lines with the smallest variance were further compared with each other using the Fischer–Snedecor test.

An intra-observer test for the precision of the measurements was performed in order to verify if the observers were equally consistent. In this step, we were interested in analysing whether there was any variability on each observer's execution regarding the measurements performed on all the test subjects for each line. First, we calculated the variance of each observer i obtained for all the test subjects, for every line k (S_{ki}^2); then, the variances S_{ki}^2 of the angles corresponding to line k were compared using the Bartlett test Eq. 4:

$$B = \frac{2.30259}{C}\left\{(n-n_i)\,.\,\ln\left(S^2\right) - \sum_{j=1}^{n_i}\left(n_j-1\right)\,.\,\ln\left(S_{ki}^2\right)\right\}$$
$$\overset{\bullet}{\cap}\ \chi^2_{(n_i-1)} \tag{4}$$

where

$$C = 1 + \frac{1}{3(i+1)}\left\{\sum_{j=1}^{i}\left(\frac{1}{n_j-1} - \frac{1}{n-1}\right)\right\}$$

n - total number of observations for each k (our case: 80)
S_{ki}^2 - intra-observer variance of the angle for line k for a given observer i
$\chi^2_{(n_i-1)}$ - theoretical value of χ^2 statistics with $(n_i-1)df$.

Results

The results regarding the variance of the four lines for each test subject ($\bar{\alpha}_{kj}$; mean ± 1 SD) as performed by the observers are presented on Table 1.

The mean variances S_k^2 corresponding to each line are shown in Table 2.

Table 3 shows the mean values corresponding to the angles measured in all subjects by every observer ($\bar{\alpha}_{ki}$; mean ± 1 SD).

Of the four lines, the line k_1 (PC-OB - Fig. 3) yield the least inter-observer variance. According to Bartlett' test, significant differences between the mean variances of the four reference lines were obtained (χ^2: χ^2 (3) = 82.54,

Table 1 Inter-observer study for the stability of the lines. $\bar{\alpha}_{kj} \pm 1$SD for α_{kij} in each reference line in every test subject j obtained by the eight observers

Test subject n°	Line k_1	Line k_2	Line k_3	Line k_4
j_1	8.4 ± 0.9	18.6 ± 2.9	18.4 ± 5.0	21.3 ± 7.6
j_2	3.4 ± 1.2	12.0 ± 2.1	24.0 ± 1.2	17.3 ± 2.3
j_3	3.8 ± 0.7	14.8 ± 2.5	18.6 ± 4.6	18.4 ± 2.9
j_4	6.9 ± 1.0	14.4 ± 2.4	14.6 ± 3.6	17.6 ± 3.5
j_5	16.1 ± 1.2	17.1 ± 3.8	27.1 ± 3.6	25.6 ± 4.3
j_6	7.5 ± 0.5	11.6 ± 1.2	18.1 ± 1.9	15.4 ± 2.8
j_7	6.9 ± 0.6	11.8 ± 1.7	17.6 ± 3.7	13.6 ± 2.5
j_8	20.1 ± 0.8	26.8 ± 1.7	27.8 ± 4.8	25.6 ± 3.4
j_9	12.3 ± 1.0	18.4 ± 1.7	24.8 ± 3.6	24.6 ± 5.0
j_{10}	9.3 ± 0.5	24.3 ± 5.6	32.8 ± 3.4	14.1 ± 7.8

$\bar{\alpha}_{kj}$ in degrees, measured with respect to the x-axis (set to zero)

Table 2 Variability for each line assessed. Mean of the variances S_k^2 in the eight observers

Line n°	S_k^2
k_1	0.8
k_2	8.1*
k_3	13.9
k_4	21.3

*significantly different from line 1 with the Fischer–Snedecor test ($p < 0.01$); Bartlett's test has shown that the variances of the groups were not equal

Table 3 Intra-observer study for the technical precision of the observers. $\bar{\alpha}_{ki} \pm 1SD$ for α_{kij} in each reference line for all test subjects obtained by the eight observers i

Observer n°	Line k_1	Line k_2	Line k_3	Line k_4
i_1	9.1 ± 5.4	16.8 ± 5.7	23.2 ± 5.4	21.8 ± 6.2
i_2	9.4 ± 5.2	18.2 ± 4.9	24.6 ± 5.2	22.9 ± 5.6
I_3	9.4 ± 5.5	16.2 ± 5.6	27.0 ± 6.2	23.9 ± 6.3
I_4	9.4 ± 5.8	16.9 ± 5.7	21.0 ± 7.5	16.8 ± 4.8
i_5	9.3 ± 5.8	16.6 ± 6.5	20.2 ± 8.1	17.3 ± 6.1
i_6	9.4 ± 5.0	17.4 ± 5.6	21.0 ± 6.1	16.5 ± 5.3
i_7	9.8 ± 4.9	16.5 ± 5.9	20.3 ± 7.3	17.9 ± 4.8
i_8	9.8 ± 5.3	17.1 ± 5.9	21.7 ± 4.6	17.7 ± 6.8

$\bar{\alpha}_{ki}$ in degrees, measured with respect to the x-axis (set to zero)

$p < 0.0001$). To further verify which line had the smallest variability, we tested the lines with the smallest variance (k_1 and k_2) using the Fischer–Snedecor test. There were significant differences between k_1 and k_2 [$F(9,9) = 103.2$, $p < 0.01$), indicating that k_1, the posterior commissure-obex line (PC-OB), has the smallest variance.

There were no significant intra-observer differences (Table 3) in the precision of the tracing for each line (Bartlett's test: $p > 0.05$ for lines $k_1 - k_4$: χ^2 for k_1: $\chi^2(7) = 0.47$, $p = 0.99$; χ^2 for k_2: $\chi^2(7) = 1.28$, $p = 0.98$; χ^2 for k_3: $\chi^2(7) = 5.49$, $p = 0.60$; χ^2 for k_4: $\chi^2(7) = 2.49$, $p = 0.93$).

Discussion

Topographic imaging provides information about individual brain structures. MRI, due to its multi-planar capabilities and high contrast resolution is a preferred method to analyse the morphometry of the core limbic structures of the temporal lobe.

In qMRI, the validity of hippocampal and amygdala quantification using volumetry, relaxometry or spectroscopy (and of para-hippocampal cortices volumetrics), depends on the quality of the images from which measurements are made.

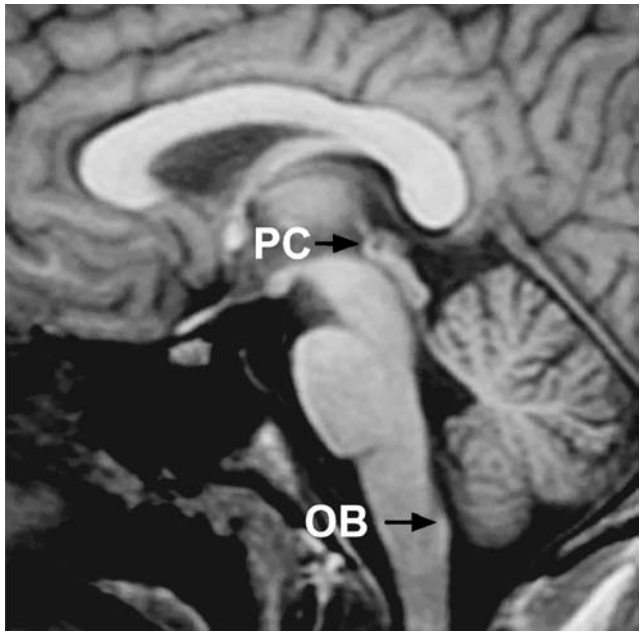

Fig. 3 Highlight of a mid-sagittal MR image showing the PC-OB anatomical details

In this study we sought to determine the stability of four sagittal reference lines, by assessing the variability of the manual tracing performed by a group of eight experienced observers in the evaluation of MR images using ten healthy controls.

Among all observers in this study, the PC-OB line showed the smallest variation while the orthogonal lines to both the right and left hippocampal axis had the largest standard deviations. These results are not surprising. In principle it is simpler to trace a line that joins two well-recognized anatomical structures, such as the posterior commissure and the obex of the IV ventricle, than an arbitrary line perpendicular to the main axis of the hippocampus, whose normal structure encompasses several cortical infoldings [26]. Further, on para-sagittal images the axis of the hippocampal head is frequently disparate to that of the body (see figures 96E and 97C in [26]). This angulation can be a source of error with respect to the choice of the appropriate orthogonal plane.

The lines tested are currently used in radiological practice as anatomical landmarks for the tilted orientation of the temporal lobe. In particular the line referred by several authors as "perpendicular to the main (or long) hippocampal axis" [10, 19, 20, 27, 28] is widely used. Also, for axial imaging the line "parallel to the longitudinal axis of the hippocampus" (obtained at right angles from the previous) is considered [14, 29]. Recently [23], the posterior commissure-obex line has been proposed as an accurate

reference to obtain angulated coronal and axial images to the main axes of the temporal lobes.

In the clinical setting it is likely that different radiologists and radiographers are responsible for the examinations of different patients. Thus, the importance of using a stable sagittal reference line as a scout for angulated planes to the temporal lobes cannot be overestimated. A simple, reproducible and well-defined anatomical landmark can contribute to the accurate comparisons of the MRI exams and increase the consistency of qMRI measurements.

Hippocampal and amygdala lesions include structural changes that disrupt their normal morphology and appearance. Moreover, the highly variable sulcal pattern of the basal and para-hippocampal temporal lobe can be an additional adverse source of variation to the imaging analysis of the subdivisions of the mesio-temporal region [30, 31]. Thus, when planning the appropriate imaging axis for the temporal lobes of a patient, it is advisable to rely on references other than the structure of interest, which may be damaged. The PC-OB line provides a stable choice since it is simple to identify and to trace. Moreover, to date, the involvement of both the posterior commissure and the obex of the IV ventricle has never been reported in the pathology of neurodegenerative disorders and TLE, which may alter their morphometry.

Conclusion

The stability and reproducibility of temporal lobe MRI can be improved by using the posterior commissure-obex line as an anatomical scout for the tilted coronal and axial sequences. Quantitative assessment of the hippocampus and amygdala, but also of the para-hippocampal cortices can benefit most from this improved stability since it predicts higher inter-observer reproducibility.

Acknowledgements This research was funded by a grant from The Science and Technology Foundation (BD 18498/98) awarded to P.M.G.P. Other support was provided by The Grünenthal Foundation. We thank the observers of the study, the Neuroradiologists Constança Jordão, Pedro Evangelista and Jorge Cannas, the Residents in Neuroradiology (at the date of the study) Teresa Palma and Carla Conceição and the Radiographers Cristina Menezes and Alfredo Raio. Alberto Leal is acknowledged for stimulating discussions regarding this project. We wish to thank Professor Fernando Lopes da Silva for his insightful comments on the manuscript.

References

1. Falconer MA, Serafetinides EA, Corsellis JAN (1964) Etiology and pathogenesis of temporal lobe epilepsy. Arch Neurol 10:233–248
2. Mouton PR, Martin LJ, Calhoun ME, Dal Forno G, Price DL (1998) Cognitive decline strongly correlates with cortical atrophy in Alzheimer's dementia. Neurobiol Aging 19:371–377
3. Amaral DG (1987) Memory: anatomical organization of candidate brain regions. In: Plum F, Mountcastle V (eds) Higher functions of the brain, handbook of physiology, Part I. Am Physiol Soc, Washington, pp211–294
4. Petersen RC, Doody R, Kurz A, et al. (2001) Current concepts in mild cognitive impairment. Arch Neurol 58:1985–1992
5. Gur RE, Turetsky BI, Cowell PE, et al. (2000) Temporolimbic volume reductions in schizophrenia. Arch Gen Psychiatry 57:769–775
6. Bigler ED, Blatter DD, Anderson CV, et al. (1997) Hippocampal volume in normal aging and traumatic brain injury. AJNR Am J Neuroradiol 18:11–23
7. Gloor P (1997) The temporal lobe and the limbic system. Oxford University Press, New York
8. Tofts PS (2003) Quantitative MRI of the brain: measuring changes caused by disease. Wiley, Chichester
9. Bronen RA, Cheung G, Charles JT, et al. (1991) Imaging findings in hippocampal sclerosis: correlation with pathology. Am J Neuroradiol 12:933–940
10. Jack CR, Petersen RC, O'Brien PC, Tangalos EG (1992) MR-based hippocampal volumetry in the diagnosis of Alzheimer's disease. Neurology 42:183–188
11. Soininen HS, Partanen K, Pitkänen A, et al. (1994) Volumetric MRI analysis of the amygdala and the hippocampus in subjects with age-associated memory impairment: correlation to visual and verbal memory. Neurology 44:1660–1668
12. Velakoulis D, Pantelis C, McGorry PD, et al. (1999) Hippocampal volume in first-episode psychoses and chronic schizophrenia: a high-resolution magnetic resonance imaging study. Arch Gen Psychiatry 56:133–141
13. Briellmann RS, Kalnins RM, Berkovic SF, Jackson GD (2002) Hippocampal pathology in refractory temporal lobe epilepsy: T2-weighted signal change reflects dentate gliosis. Neurology 58:265–271
14. Ng TC, Comair YG, Xue M, et al. (1994) Temporal lobe epilepsy: presurgical localization with proton chemical shift imaging. Radiology 193:465–472
15. Oppenheim C, Dormont D, Biondi A, et al. (1998) Loss of digitations of the hippocampal head on high-resolution fast spin-echo MR: a sign of mesial temporal sclerosis. AJNR Am J Neuroradiol 19:457–463
16. Jackson GD (1995) The diagnosis of hippocampal sclerosis: other techniques. Magn Reson Imaging 13:1081–1093
17. Kim JH, Tien RD, Felsberg GJ, Osumi AK, Lee N (1995) Clinical significance of asymmetry of the fornix and mamillary body on MR in hippocampal sclerosis. AJNR Am J Neuroradiol 16:509–515
18. Jack CR Jr, Rydberg CH, Krecke KN, et al. (1996) Mesial temporal sclerosis: diagnosis with fluid-attenuated inversion-recovery versus spin-echo MR imaging. Radiology 199:367–373
19. Achten E, Boon P, De Poorter J, et al. (1995) An MR protocol for presurgical evaluation of patients with complex partial seizures of temporal lobe origin. AJNR Am J Neuroradiol 16:1201–1213
20. Watson C, Andermann F, Gloor P, et al. (1992) Anatomic basis of amygdaloid and hippocampal volume measurement by magnetic resonance imaging. Neurology 42:1743–1750

21. Meiners LC, Valk J, van Gils PG, et al. (1997) Assessment of the preferred plane and sequence in the depiction of mesial temporal sclerosis using magnetic resonance imaging. Invest Radiol 32:268–276
22. Jackson GD, Connelly A, Duncan JS, Grunewald RA, Gadian DG (1993) Detection of hippocampal pathology in intractable partial epilepsy: increased sensitivity with quantitative magnetic resonance T2 relaxometry. Neurology 43:1793–1799
23. Tamraz JC, Comair YG (2000) Cephalic reference lines suitable for neuroimaging. In: Tamraz JC, Comair YG (eds) Atlas of regional anatomy of the brain using MRI – with functional correlations. Springer, Berlin Heidelberg New York, pp.11–50
24. Bartlett PA, Richardson MP, Duncan JS (2002) Measurement of amygdala T2 relaxation time in temporal lobe epilepsy. J Neurol Neurosurg Psychiatry 73:753–755
25. Folstein MF, Folstein SE, McHugh PR (1975) "Mini-mental state". A practical method for grading the cognitive state of patients for the clinician. J Psychiatr Res 12:189–198
26. Duvernoy HM (1998) The human hippocampus. Functional anatomy, vascularization and serial sections with MRI. Springer, Berlin Heidelberg New York
27. Du AT, Schuff N, Amend D, et al. (2001) Magnetic resonance imaging of the entorhinal cortex and hippocampus in mild cognitive impairment and Alzheimer's disease. J Neurol Neurosurg Psychiatry 71:441–447
28. Von Oertzen J, Urbach H, Jungbluth S, et al. (2002) Standard magnetic resonance imaging is inadequate for patients with refractory focal epilepsy. J Neurol Neurosurg Psychiatry 73:643–647
29. Capizzano AA, Vermathen P, Laxer KD, et al. (2001) Temporal lobe epilepsy: qualitative reading of 1H MR spectroscopic images for presurgical evaluation. Radiology 218:144–151
30. Novak K, Czech T, Prayer D, et al. (2002) Individual variations in the sulcal anatomy of the basal temporal lobe and its relevance for epilepsy surgery: an anatomical study performed using magnetic resonance imaging. J Neurosurg 96:464–473
31. Insausti R, Juottonen K, Soininen H, et al. (1998) MR volumetric analysis of the human entorhinal, perirhinal, and temporopolar cortices. AJNR Am J Neuroradiol 19:659–671